

# Capacity Performance of Wireless OAM-Based Massive MIMO System

Fuchun Mao<sup>1</sup>, Ming Huang<sup>1, \*</sup>, Jingjing Yang<sup>1</sup>,  
Chengfu Yang<sup>1</sup>, Tinghua Li<sup>2</sup>, and Jialin Zhang<sup>3</sup>

**Abstract**—Orbital angular momentum (OAM) as a powerful candidate to enhance the spectral efficiency and system capacity by providing the new degree of freedom for multiplexing has been recently advocated in wireless communications. In this paper, we propose an OAM-based massive multiple-input multiple-output (MIMO) scheme to significantly improve the transmission performance of wireless communication system in line-of-sight scene. The uniform rectangular arrays (URAs) are used as transceivers in our system model, and the ideal OAM antenna model that is capable of providing OAM-channel independently is used as the array element. Multiple reference coordinate systems based on per transmitting antenna and the cumulative phase of specific radio vortices are used to describe the OAM-MIMO channel model. The results of numerical analysis indicate that the proposed OAM-based massive MIMO system could obtain an overwhelming capacity gain against the conventional MIMO system.

## 1. INTRODUCTION

The orbital angular momentum (OAM) of electromagnetic fields characterized by the spiral phase factor of  $\exp(jl\varphi)$  is considered a new degree of freedom for multiplexing, where  $l$  and  $\varphi$  represent the mode number of OAM waves and the azimuth, respectively [1, 2]. This is of great significance to the telecommunications industry as indicated in Fig. 1, which describes only six degrees of freedom for multiple access, namely the time, frequency, code sequence, space, polarization, and OAM state. They have been deeply developed and utilized at present, except for the OAM state. Hopefully, several validated experimental reports are available in optics [3], millimeter wave [4, 5], and radio frequency [6–9]. Due to good collimation, OAM-based communication performs much better in optical and millimeter bands than in the radio frequency. What is worse, some initial reports suggest that OAM is just a subset of MIMO technology and does not give any additional capacity gain [10, 11]. The reason for this conclusion is that the presented uniform circular array (UCA) is treated as an OAM generator that only produces a single OAM channel during a time slot. Thus the argued capacity limit of UCA system is indeed the production limit of OAM carriers. Recent researches show more positive results about OAM increasing the channel capacity [12, 13].

As the basis for performance analysis, the channel matrix of wireless OAM-MIMO systems with various array configurations has been studied, such as the typical UCA system [14, 15], misalignment UCA system [16], nested UCA system [17], fractal UCA system [18], and uniform line array (ULA) systems [19, 20]. In spite of offering some inspirations, these reports do not use reference coordinates in analysis process, which is actually of significance due to the extreme spatial coordinate dependence

---

Received 7 March 2019, Accepted 23 June 2019, Scheduled 2 July 2019

\* Corresponding author: Ming Huang (huangming@ynu.edu.cn).

<sup>1</sup> School of Information Science and Engineering, Wireless Innovation Lab of Yunnan University, Kunming, Yunnan 650091, China.

<sup>2</sup> The Technical Center of China Tobacco Yunnan Industrial Co. Ltd., Kunming, Yunnan 650231, China. <sup>3</sup> Radio Monitoring Center of Yunnan Province, Kunming, Yunnan 650228, China.

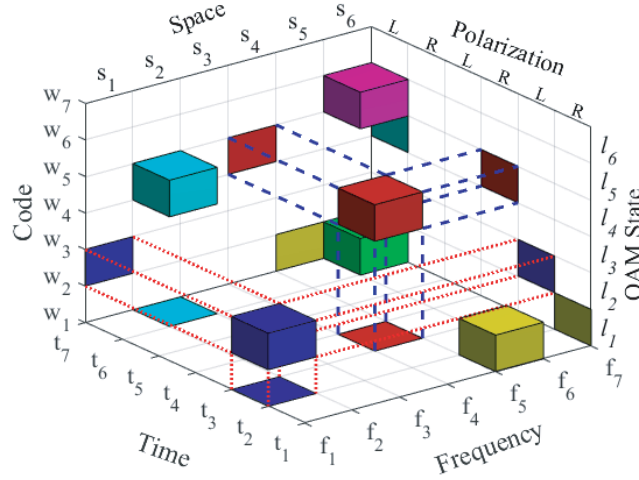


**Figure 1.** The map of resource lattice for multiplexing. Here  $f$ ,  $t$ ,  $w$ ,  $s$ , and  $l$  represent frequency-, time-, code-, space-, and OAM-channel in turn;  $R$  and  $L$  are right-hand and left-hand circular polarization, respectively.

of OAM fields. In addition, the use of non-OAM antenna model as array element causes some of the above reports to fail to observe the expected capacity gain.

In this paper, we consider an OAM-based massive MIMO system for the line-of-sight wireless communications, in which both the transmitter and receiver consist of a URA. An ideal OAM antenna that is capable of generating OAM wave is used as the transmit-receive antenna in URAs. The relevant wireless channel model is deduced theoretically. Then, the capacity performance of the proposed OAM-based massive MIMO system is performed. The numerical simulation shows some exciting results.

## 2. SYSTEM MODEL

The proposed OAM-based massive MIMO system is shown in Fig. 2(a), where  $D$  is the space between transmitter and receiver;  $\Delta$  is the space among adjacent elements in URAs;  $d_{mn}$  denotes the propagation distance from the  $n$ -th transmitting antenna  $T_n$  to the  $m$ -th receiving antenna  $R_m$ ; and  $\phi_{mn}$  represents the initial azimuth of  $R_m$  referencing to  $T_n$ .  $R'_m$  is the normal projection of  $R_m$ . As depicted in Fig. 2(b), we code the antennas with  $n(p_t, q_t)$  in the transmitter and  $m(p_r, q_r)$  in receiver for the convenience of

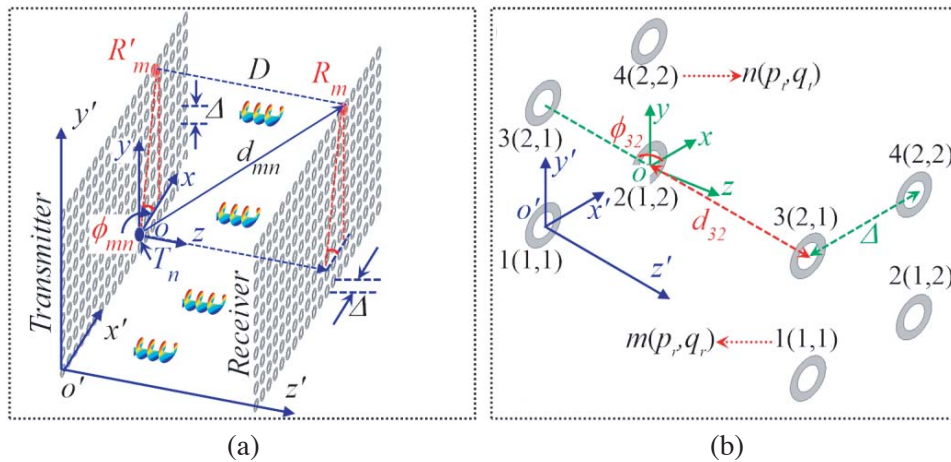


**Figure 2.** The OAM-based massive MIMO system. (a) Generalized  $M \times N$  case. (b) Simplified  $4 \times 4$  case.

subsequent analysis. Here  $p_t$  and  $p_r$  denote the serial number of rows in the URAs, while  $q_t$  and  $q_r$  represent the serial number of columns, respectively. In addition,  $o'-x'y'z'$  is the original coordinate system for the whole system, while  $o-xyz$  is the reference coordinate system of  $T_n$ . The transformation relationship between them is given below

$$x = x' - (q_t - 1)\Delta, \quad y = y' - (p_t - 1)\Delta, \quad z = z' \quad (1)$$

The reason for applying the reference coordinates is the intrinsic spatial dependence of OAM fields. The azimuthal angle  $\varphi$  in spiral phase factor  $\exp(jl\varphi)$  has to be the angular coordinate around the beam-axis of OAM waves. In other words,  $\varphi$  has to be defined by  $o-xyz$  rather than  $o'-x'y'z'$ . In such an OAM-based massive MIMO system, the received signals can be expressed as

$$\mathbf{Y} = \mathbf{H}\mathbf{X} + \mathbf{n} \quad (2)$$

Here  $\mathbf{Y} = [y_1, \dots, y_i, \dots, y_M]^T$  is the received signal vector, in which  $y_i = \sum_j^N h_{ij}\tilde{x}_j + n_i$  is the signals and noise obtained by the  $i$ -th receiving antenna.  $\mathbf{X} = [\tilde{x}_1, \dots, \tilde{x}_i, \dots, \tilde{x}_N]^T$  is the transmitted signals with  $\tilde{x}_j = [l_1, \dots, l_k, \dots, l_Q]^T$  denoting the OAM signals modulated by the  $j$ -th transmitting antenna, where  $l_k$  is the channel label of certain OAM signal.  $\mathbf{n} = [n_1, \dots, n_i, \dots, n_M]^T$  is the complex Gauss white noise vector introduced by the wireless link.  $\mathbf{H} = [\mathbf{h}_1, \dots, \mathbf{h}_j, \dots, \mathbf{h}_N]^T$  is the channel matrix with  $\mathbf{h}_j$  representing the channel response vector between the  $j$ -th transmitting antenna and all receiving antennas. When the channel state information (CSI) of the system is known, an optimal power allocation will be applied at the transmitter. According to the Shannon's channel capacity theorem, the capacity of the proposed OAM-based massive MIMO system can be expressed as

$$C = \sum_j^\gamma \log_2 \left( 1 + \frac{P_j}{\sigma^2/\delta_j^2} \right) \text{ bps/Hz} \quad (3)$$

Here  $\gamma$  and  $\delta_j$  are the rank and singular value of channel matrix, respectively.  $\sigma$  is the variance of noise.  $p_j$  is the sub-power allocated by the water-filling principle.

### 3. CHANNEL MODEL

The transfer function from  $T_n$  to  $R_m$  can be considered as the MIMO response superimposed by a spiral phase term [14], and expressed as follows

$$h_{mn} = h_{mn}^{\text{mimo}} \cdot h_{mn}^{\text{oam}} = \frac{\lambda\beta}{4\pi d_{mn}} e^{-j\frac{2\pi}{\lambda}d_{mn}} \cdot e^{j\tilde{l}_n\tilde{\varphi}_{mn,l}} \quad (4)$$

Here  $\beta$  is a constant containing attenuation and phase caused by antennas and their patterns on both sides [10];  $\lambda$  denotes the wavelength;  $\tilde{l}_n = l_1, \dots, l_Q$  contains all OAM fields generated by  $T_n$ ; and  $\tilde{\varphi}_{mn,l}$  denotes the cumulative phases of the  $l$ -labeled OAM carrier after propagating from  $T_n$  to  $R_m$ .

The channel matrix of the proposed OAM-based massive MIMO system is completely determined by Eq. (4), in which only  $d_{mn}$  and  $\tilde{\varphi}_{mn,l}$  are pending. According to Fig. 2(a), the propagation distance  $d_{mn}$  can be calculated by

$$d_{mn} = \text{sqrt} \left\{ D^2 + [(p_t - p_r) \times \Delta]^2 + [(q_t - q_r) \times \Delta]^2 \right\} \quad (5)$$

and the cumulative phases  $\tilde{\varphi}_{mn,l}$  can be performed by

$$\tilde{\varphi}_{mn,l} = \phi_{mn} + 2\pi \cdot \tilde{l}_n \cdot \frac{D}{\lambda} \quad (6)$$

The initial phase  $\phi_{mn}$  depends on only the relative position relationship between  $T_n$  and  $R_m$ , and is

equal for all  $\tilde{l}_n$  OAM carriers. It can be calculated by

$$\phi_{mn} = \begin{cases} \arctan(|p_t - p_r|/|q_t - q_r|), & p_r > p_t, q_r > q_t \\ \pi - \arctan(|p_t - p_r|/|q_t - q_r|), & p_r > p_t, q_r < q_t \\ \pi + \arctan(|p_t - p_r|/|q_t - q_r|), & p_r < p_t, q_r < q_t \\ 2\pi - \arctan(|p_t - p_r|/|q_t - q_r|), & p_r < p_t, q_r > q_t \\ 0, & p_r = p_t, q_r \geq q_t \\ \pi/2, & p_r > p_t, q_r = q_t \\ \pi, & p_r = p_t, q_r < q_t \\ 3\pi/2, & p_r < p_t, q_r = q_t \end{cases} \quad (7)$$

In order to simplify the formulas without loss the generality, we consider the simple case of each transmitting antenna generating only a single OAM carrier, and the topological charge of the generated radio OAM carrier equals its own serial number, namely  $\tilde{l}_n = n$ .

## 4. CAPACITY ANALYSIS AND SIMULATION

### 4.1. Conventional MIMO System

To show more details about the capacity analysis on the proposed OAM-based massive MIMO system, we begin with a  $4 \times 4$  URA based system as depicted in Fig. 2(b). The matrix of propagation distance can be obtained by using Eq. (5) below

$$\mathbf{d} = \begin{bmatrix} d_{11} & d_{12} & d_{13} & d_{14} \\ d_{21} & d_{22} & d_{23} & d_{24} \\ d_{31} & d_{32} & d_{33} & d_{34} \\ d_{41} & d_{42} & d_{43} & d_{44} \end{bmatrix} = \begin{bmatrix} D & d_1 & d_1 & d_2 \\ d_1 & D & d_2 & d_1 \\ d_1 & d_2 & D & d_1 \\ d_2 & d_1 & d_1 & D \end{bmatrix} \quad (8)$$

where  $d_1 = (D^2 + \Delta^2)^{1/2}$ , and  $d_2 = (D^2 + 2\Delta^2)^{1/2}$ . The symmetry of  $\mathbf{d}$  may be useful in reducing the computational complexity. Substituting Eq. (8) into Eq. (4) and making  $h_{mn}^{oam} = 1$ , the channel matrix for conventional MIMO system can be written as

$$\mathbf{H}_{\text{mimo}} = \frac{\lambda\beta}{4\pi} \begin{bmatrix} e^{-jkD/D} & e^{-jkd_1/d_1} & e^{-jkd_1/d_1} & e^{-jkd_2/d_2} \\ e^{-jkd_1/d_1} & e^{-jkD/D} & e^{-jkd_2/d_2} & e^{-jkd_1/d_1} \\ e^{-jkd_1/d_1} & e^{-jkd_2/d_2} & e^{-jkD/D} & e^{-jkd_1/d_1} \\ e^{-jkd_2/d_2} & e^{-jkd_1/d_1} & e^{-jkd_1/d_1} & e^{-jkD/D} \end{bmatrix}. \quad (9)$$

where  $k = 2\pi/\lambda$ .

### 4.2. OAM-Based MIMO System

The channel matrix of the  $4 \times 4$  URAs-based OAM-MIMO system is obtained by applying Eq. (4) as

$$\mathbf{H} = \frac{\beta\lambda}{4\pi} \begin{bmatrix} \frac{e^{-jkD-j\varphi_{11}}}{D} & \frac{e^{-jkd_1-j2\varphi_{12}}}{d_1} & \frac{e^{-jkd_1-j3\varphi_{13}}}{d_1} & \frac{e^{-jkd_2-j4\varphi_{14}}}{d_2} \\ \frac{e^{-jkd_1-j\varphi_{21}}}{d_1} & \frac{e^{-jkD-j2\varphi_{22}}}{D} & \frac{e^{-jkd_2-j3\varphi_{23}}}{d_2} & \frac{e^{-jkd_1-j4\varphi_{24}}}{d_1} \\ \frac{e^{-jkd_1-j\varphi_{31}}}{d_1} & \frac{e^{-jkd_2-j2\varphi_{32}}}{d_2} & \frac{e^{-jkD-j3\varphi_{33}}}{D} & \frac{e^{-jkd_1-j4\varphi_{34}}}{d_1} \\ \frac{e^{-jkd_2-j\varphi_{41}}}{d_2} & \frac{e^{-jkd_1-j2\varphi_{42}}}{d_1} & \frac{e^{-jkd_1-j3\varphi_{43}}}{d_1} & \frac{e^{-jkD-j4\varphi_{44}}}{D} \end{bmatrix} \quad (10)$$

where  $\varphi_{mn}$  is ruled by Eq. (6) with  $\tilde{l}_n = n$ . According to Eq. (7) and Fig. 2(b), the initial phase matrix  $\phi$  is obtained as

$$\phi = \begin{bmatrix} \phi_{11} & \phi_{12} & \phi_{13} & \phi_{14} \\ \phi_{21} & \phi_{22} & \phi_{23} & \phi_{24} \\ \phi_{31} & \phi_{32} & \phi_{33} & \phi_{34} \\ \phi_{41} & \phi_{42} & \phi_{43} & \phi_{44} \end{bmatrix} = \begin{bmatrix} 0 & \pi & 3\pi/2 & 5\pi/4 \\ 0 & 0 & 7\pi/4 & 3\pi/2 \\ \pi/2 & 3\pi/4 & 0 & \pi \\ \pi/4 & \pi/2 & 0 & 0 \end{bmatrix} \quad (11)$$

Substituting Eq. (11) and Eq. (6) into Eq. (10), the channel matrix for the  $4 \times 4$  URAs based OAM-MIMO system can be obtained as

$$\mathbf{H} = \frac{\beta\lambda}{4\pi} \begin{bmatrix} \frac{1}{D} & \frac{e^{-jk(d_1-4D)}}{d_1} & \frac{je^{-jk(d_1-9D)}}{d_1} & \frac{-e^{-jk(d_2-16D)}}{d_2} \\ \frac{e^{-jk(d_1-D)}}{d_1} & \frac{e^{j3kD}}{D} & \frac{e^{-jk(d_2-9D)}e^{j21\pi/4}}{d_2} & \frac{e^{-jk(d_1-16D)}}{d_1} \\ \frac{je^{-jk(d_1-D)}}{d_1} & \frac{-je^{-jk(d_2-4D)}}{d_2} & \frac{e^{j8kD}}{D} & \frac{e^{-jk(d_1-16D)}}{d_1} \\ \frac{e^{-jk(d_2-D)} \cdot e^{j\pi/4}}{d_2} & \frac{-e^{-jk(d_1-4D)}}{d_1} & \frac{e^{-jk(d_1-9D)}}{d_1} & \frac{e^{j15kD}}{D} \end{bmatrix} \quad (12)$$

### 4.3. Simulation Results

In this section, both the conventional massive MIMO and OAM-based massive MIMO are discussed in wireless line-of-sight scenario. To observe the capacity performance of the simplified  $4 \times 4$  URAs based system, the main simulation parameters are set as below: the carrier frequency and corresponding carrier wavelength are 66 GHz and 4.55 mm, respectively; the gain coefficient  $\beta$  equals 40 dB; the transmitting power is 1 W; the signal-noise-rates (SNR) are 10 dB and 30 dB, respectively; the space among adjacent elements  $\Delta$  takes  $20\lambda$ . The OAM state of transmitting antennas is set by  $\tilde{l}_n = n$ , namely, the 1st, 2nd, 3rd, and 4th transmitting antennas radiate the OAM carriers with the topological charge of 1, 2, 3, and 4 in order.

Figure 3(a) depicts the capacity performance of the  $4 \times 4$  URAs based conventional MIMO system and OAM-MIMO system, with the space between transmitter and receiver  $D$  varying from  $100\lambda$  to  $20000\lambda$ . Obviously, the OAM-MIMO system shows a better capacity performance than the conventional MIMO system. For instance, at the propagation distance of  $D = 10310\lambda$ , the OAM-MIMO system

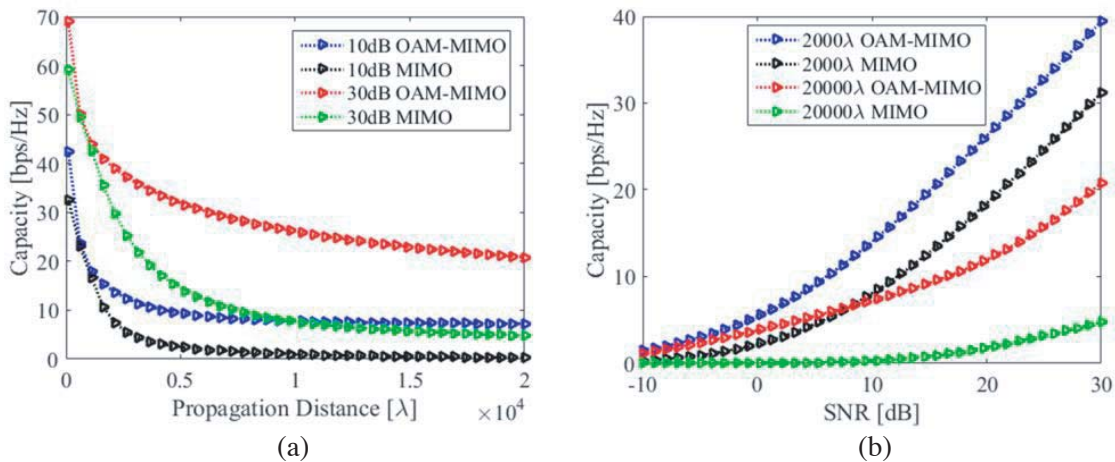


**Figure 3.** The capacity performances of  $4 \times 4$  URAs based systems versus: (a) propagation distance, (b) SNR.

obtains a channel capacity of 25.82 bps/Hz and 7.744 bps/Hz corresponding to SNR = 30 dB and SNR = 10 dB, respectively. The conventional MIMO system's channel capacities are 7.455 bps/Hz and 0.9715 bps/Hz with the same setting, which are only 28.87% and 12.55% of the OAM-MIMO system, respectively. Fig. 3(b) shows the capacity performances of the two systems over an SNR region of  $-10$  dB  $\sim$  30 dB, with the propagation distances taking  $2000\lambda$  and  $20000\lambda$ , respectively. We can draw the conclusion that is consistent with Fig. 3(a). Taking SNR = 20 dB as an example, we can see from Fig. 3(b) that the conventional MIMO obtains a channel capacity of 1.765 bps/Hz at  $D = 20000\lambda$  and 18.15 bps/Hz at  $D = 2000\lambda$ , while the channel capacity of the OAM-MIMO is 11.82 bps/Hz and 25.91 bps/Hz at the same setting. The OAM-MIMO performs 6.7 times and 1.43 times better than the conventional MIMO, respectively. This infers that the conventional MIMO is capable of promoting multiplicative capacity gain by joining the OAM techniques, and the capacity gain increases significantly with the increase of propagation distance and the decrease of SNR.

According to the theory of the massive MIMO system, no matter the conventional case or the OAM based case, the capacity performance will be enhanced significantly with the used transmitting-receiving elements increasing. This is revealed by Fig. 4, in which the propagation distance is  $5000\lambda$ ; the space among adjacent elements is  $5\lambda$ ; the  $n$ -th transmitting antenna radiates the  $n$ -labeled OAM carrier; and the used antennas are  $4 \times 4$ ,  $9 \times 9$ ,  $16 \times 16$ ,  $32 \times 32$ ,  $64 \times 64$ ,  $100 \times 100$  in order. The transmitting power is 1 W. Taking SNR = 30 dB into account, the channel capacities with the used elements ascending are 8.737, 12.85, 19.6, 33.65, 53.48, 78.86 (bps/Hz) for the conventional massive MIMO systems, and 24.58, 61.97, 119, 299.1, 587.5, 973.8 (bps/Hz) for the proposed OAM-based massive MIMO systems, and 4.719 (bps/Hz) for the single-input single-output (SISO) system. Therefore, the OAM-based massive MIMO is orderly more excellent than the conventional massive MIMO 2.813 times, 4.823 times, 6.072 times, 8.89 times, 10.99 times, and 12.35 times, and much more overwhelming than SISO system.

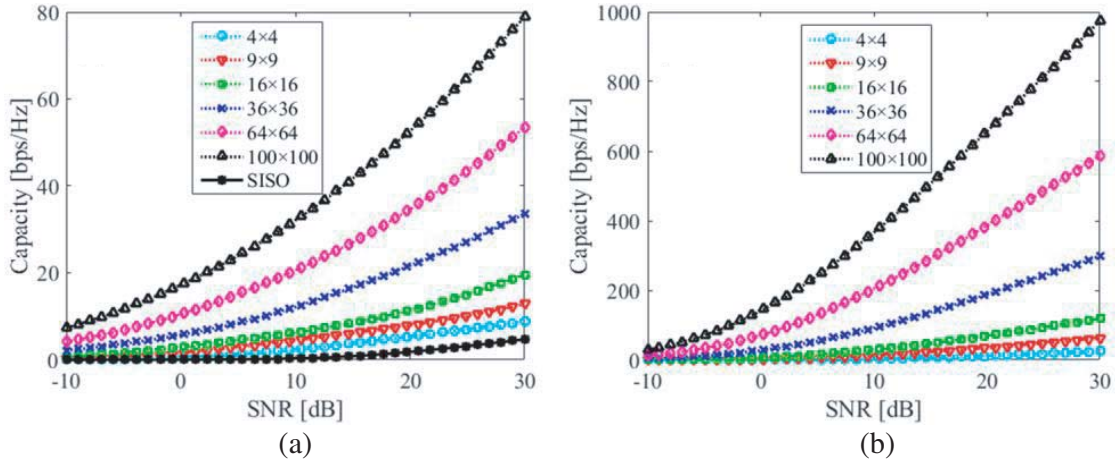


**Figure 4.** The capacity performance of: (a) conventional massive MIMO system and SISO system; (b) the proposed OAM-based massive MIMO system.

## 5. CONCLUSIONS

We propose an OAM-based massive MIMO system for the line-of-sight wireless communications. The URAs and OAM antennas are respectively used as transceivers and transmitting-receiving antennas in this paper. Multiple reference coordinate systems are used to correctly describe the OAM-MIMO channel model. Channel matrixes and capacity analyses for the OAM-based massive MIMO and conventional massive MIMO are deduced theoretically and performed numerically. The results of simulation show a significant enhancement of channel capacity in the proposed OAM-MIMO system by comparing with the conventional MIMO system and SISO system.

## ACKNOWLEDGMENT

This work was supported by the National Natural Science Foundation of China (Grant Nos. 61461052, 61863035, 11564044), the Seventh of Yunnan University Graduate Student Scientific Research Project (Grant No. ynuy201443), and the doctoral award for the academic newcomers (2014) of Yunnan Province.

## REFERENCES

1. Djordjevic, I. B., "Multidimensional OAM-based secure high-speed wireless communications," *IEEE Access*, Vol. 5, 16416–16428, 2017.
2. Mao, F. C., M. Huang, C. F. Yang, T. H. Li, J. L. Zhang, and S. Y. Chen, "Orbital angular momentum generation using circular ring resonators in radio frequency," *Chinese Phys. Lett.*, Vol. 35, No. 2, 020701, 2018.
3. Ren, Y. X., Z. Wang, P. C. Liao, L. Li, G. D. Xie, H. Huang, Z. Zhao, Y. Yan, N. Ahmed, A. Willner, M. P. J. Lavery, N. Ashrafi, S. Ashrafi, R. Bock, M. Tur, I. B. Djordjevic, M. A. Neifeld, and A. E. Willner, "Experimental characterization of a 400 Gbit/s orbital angular momentum multiplexed free-space optical link over 120 m," *Opt. Lett.*, Vol. 41, No. 3, 622–625, 2016.
4. Yan, Y., G. D. Xie, M. P. J. Lavery, H. Huang, N. Ahmed, C. J. Bao, Y. X. Ren, Y. W. Gao, L. Li, Z. Zhao, A. F. Molisch, M. Tur, M. J. Padgett, and A. E. Willner, "High-capacity millimeter-wave communications with orbital angular momentum multiplexing," *Nat. Commun.*, Vol. 5, 4876, 2014.
5. Shi, Y. and Y. Zhang, "Generation of wideband tunable orbital angular momentum vortex waves using graphene metamaterial reflectarray," *IEEE Access*, Vol. 6, 5341–5347, 2018.
6. Tamburini, F., E. Mari, G. Parisi, F. Spinello, M. Oldoni, R. A. Ravanelli, P. Coassini, C. G. Someda, B. Thidé, and F. Romanato, "Tripling the capacity of a point-to-point radio link by using electromagnetic vortices," *Radio Sci.*, Vol. 50, No. 6, 501–508, 2015.
7. Yu, S. X., L. Li, G. M. Shi, C. Zhu, and Y. Shi, "Generating multiple orbital angular momentum vortex beams using a metasurface in radio frequency domain," *Appl. Phys. Lett.*, Vol. 108, No. 24, 241901, 2016.
8. Mao, F., M. Huang, T. Li, J. Zhang, and C. Yang, "Broadband generation of orbital angular momentum carrying beams in RF regimes," *Progress In Electromagnetics Research*, Vol. 160, 19–27, 2017.
9. Yu, S. X., L. Li, G. M. Shi, C. Zhu, X. X. Zhou, and Y. Shi, "Design, fabrication, and measurement of reflective metasurface for orbital angular momentum vortex wave in radio frequency domain," *Appl. Phys. Lett.*, Vol. 108, No. 12, 121903, 2016.
10. Edfors, O. and A. J. Johansson, "Is orbital angular momentum (OAM) based radio communication an unexploited area?," *IEEE Trans. Antenn. Propag.*, Vol. 60, No. 2, 1126–1131, 2012.
11. Cagliero, A. and R. Gaffoglio, "On the spectral efficiency limits of an OAM-based multiplexing scheme," *IEEE Antenn. Wirel. Pr.*, Vol. 16, 900–903, 2016.
12. Cheng, W. C., H. L. Zhang, L. P. Liang, H. Y. Jing, and Z. Li, "Orbital-angular-momentum embedded massive MIMO: Achieving multiplicative spectrum-efficiency for mmWave communications," *IEEE Access*, Vol. 6, 2732–2745, 2017.
13. Zheng, S. L., R. F. Dong, Z. F. Zhang, X. B. Yu, X. F. Jin, H. Chi, Z. N. Chen, and X. M. Zhang, "Non-line-of-sight channel performance of plane spiral orbital angular momentum MIMO systems," *IEEE Access*, Vol. 5, 25377, 2017.
14. Zhu, Q. B., T. Jiang, D. M. Qu, D. Chen, and N. R. Zhou, "Radio vortex multiple-input multiple-output communication systems with high capacity," *IEEE Access*, Vol. 3, 2456, 2015.
15. Lei, W., F. Jiang, Z. Yuan, J. Yang, G. Gui, and H. Sari, "Mode division multiple access: A new scheme based on orbital angular momentum in millimeter wave communications for fifth generation," *IET Commun.*, Vol. 12, No. 12, 1416–1421, 2018.
16. Chen, R., H. Xu, M. Moretti, and J. D. Li, "Beam steering for the misalignment in UCA-based OAM communication systems," *IEEE Wirel. Commun. Lett.*, Vol. 7, No. 4, 582585, 2018.

17. Opare, K., Y. Kuang, and J. Kponyo, "Mode combination in an ideal wireless OAM-MIMO multiplexing system," *IEEE Wirel. Commun. Lett.*, Vol. 4, No. 4, 449–452, 2015.
18. Zhao, L. J., H. L. Zhang, and W. C. Cheng, "Fractal uniform circular arrays based multi-orbital-angular-momentum-mode multiplexing vortex radio MIMO," *China Commun.*, Vol. 15, No. 9, 126–143, 2018.
19. Wang, L., X. H. Ge, R. Zi, and C. X. Wang, "Capacity analysis of orbital angular momentum wireless channels," *IEEE Access*, Vol. 5, 23069–23077, 2017.
20. Ge, X. H., R. Zi, X. S. Xiong, Q. Li, and L. Wang, "Millimeter wave communications with OAM-SM scheme for future mobile networks," *IEEE J. Sel. Area. Comm.*, Vol. 35, No. 9, 2163–2177, 2017.